Alternative polyadenylation drives oncogenic gene expression in pancreatic ductal adenocarcinoma

Swati Venkat, Arwen A Tisdale, Johann R Schwarz, et al.

Genome Res. published online February 6, 2020
Access the most recent version at doi:10.1101/gr.257550.119

Alternative polyadenylation drives oncogenic gene expression in pancreatic ductal adenocarcinoma

Swati Venkat[1], Arwen A. Tisdale[1], Johann R. Schwarz[1], Abdulrahman A. Alahmari[1], H. Carlo Maurer[2], Kenneth P. Olive[3], Kevin H. Eng[4,5] and Michael E. Feigin[1,*]

[1]Department of Pharmacology and Therapeutics, Roswell Park Comprehensive Cancer Center, Buffalo, NY
[2]Klinikum rechts der Isar, II. Medizinische Klinik, Technische Universität München, 81675, Munich, Germany
[3]Herbert Irving Comprehensive Cancer Center, Department of Medicine, Division of Digestive and Liver Diseases, Department of Pathology and Cell Biology, Columbia University Medical Center, New York, NY
[4]Department of Cancer Genetics and Genomics, Roswell Park Comprehensive Cancer Center, Buffalo, NY
[5]Department of Biostatistics and Bioinformatics, Roswell Park Comprehensive Cancer Center, Buffalo, NY

*Correspondence may be addressed to: MEF (michael.feigin@roswellpark.org), Twitter: @TheFeiginLab

Running head: APA events in pancreatic cancer

Keywords: alternative polyadenylation, pancreatic cancer, 3' untranslated region, casein kinase 1 alpha, gene regulation

ABSTRACT

Alternative polyadenylation (APA) is a gene regulatory process that dictates mRNA 3' UTR length, resulting in changes in mRNA stability and localization. APA is frequently disrupted in cancer and promotes tumorigenesis through altered expression of oncogenes and tumor suppressors. Pan-cancer analyses have revealed common APA events across the tumor landscape; however, little is known about tumor type-specific alterations that may uncover novel events and vulnerabilities. Here we integrate RNA-sequencing data from the Genotype-Tissue Expression (GTEx) project and The Cancer Genome Atlas (TCGA) to comprehensively analyze APA events in 148 pancreatic ductal adenocarcinomas (PDAs). We report widespread, recurrent and functionally relevant 3' UTR alterations associated with gene expression changes of known and newly identified PDA growth-promoting genes and experimentally validate the effects of these APA events on protein expression. We find enrichment for APA events in genes associated with known PDA pathways, loss of tumor-suppressive miRNA binding sites, and increased heterogeneity in 3' UTR forms of metabolic genes. Survival analyses reveal a subset of 3' UTR alterations that independently characterize a poor prognostic cohort among PDA patients. Finally, we identify and validate the casein kinase CSNK1A1 (also known as CK1alpha or CK1a) as an APA-regulated therapeutic target in PDA. Knockdown or pharmacological inhibition of CSNK1A1 attenuates PDA cell proliferation and clonogenic growth. Our single-cancer analysis reveals APA as an underappreciated driver of pro-tumorigenic gene expression in PDA via the loss of miRNA regulation.

INTRODUCTION

Pancreatic ductal adenocarcinoma (PDA) is a lethal cancer with a 5-year survival rate of 9% (Noone et al. 2019). Extensive sequencing studies have uncovered recurrently mutated genes (*KRAS, TP53, SMAD4, CDKN2A*) and dysregulated pathways (axon guidance, cell adhesion, small GTPase signaling, protein metabolism) driving disease initiation and progression (Jones et al. 2008; Waddell et al. 2015; Raphael et al. 2017). Gene expression profiles from hundreds of patient samples have allowed the identification of several PDA subtypes, with implications for treatment response and patient outcome (Maurer et al. 2019; Lomberk et al. 2018; Tiriac et al. 2018; Bailey et al. 2016; Moffitt et al. 2015; Collisson et al. 2011). Gene expression can be dysregulated in cancer through a variety of mechanisms, including genomic amplification/deletion, epigenetic modification and noncoding mutations in promoters/enhancers (D Antonio et al. 2017; Rheinbay et al. 2017; Jones et al. 2015; Weinhold et al. 2014; Khurana et al. 2013). For example, recurrent noncoding mutations in PDA are enriched in promoters of cancer-associated genes and pathways (Feigin et al. 2017). However, our understanding of the mechanisms driving dysregulated gene expression in cancer remains incomplete. Determining the regulatory mechanisms driving dysregulated gene expression is critical to understanding disease pathogenesis. One such regulatory mechanism that has recently gained recognition as a critical driver of gene expression is alternative polyadenylation (APA).

APA is a post-transcriptional process that generates distinct mRNA isoforms of the same gene as a mechanism to modulate gene expression. This includes transcripts that have identical coding sequences but vary only in the length of their 3' untranslated region (UTR) (Gruber and Zavolan 2019; Elkon et al. 2013; Erson-Bensan and Can 2016). Changes in 3’ UTR length can modulate mRNA stability, function or subcellular localization through disruption of miRNA or RNA-binding protein regulation (Tian and Manley 2017; Mayr 2016; Elkon et al. 2013). APA is driven by a large complex of polyadenylation factors that recognize a series of highly conserved sequences within the 3’ UTR on the newly synthesized pre-mRNA before cleavage and addition of the poly(A) tail (Elkon et al. 2013; Shi and Manley 2015; Proudfoot 2011). As most transcripts contain multiple polyadenylation sites (PAS), the choice of where to cleave is a critical determinant of 3’ UTR length. In humans, a majority of genes (51-79%) express alternative 3’ UTRs, demonstrating the widespread nature of this process (Mayr 2018). Indeed, APA has roles in muscle stem cell function, cell proliferation, chromatin signaling, pluripotent cell fate, cellular senescence and other physiological processes (Brumbaugh et al. 2018; Lackford et al. 2014; Boutet et al. 2012; Sandberg et al. 2008; Chen et al. 2018a). Recently, dysregulation of APA

has gained recognition as a driver of tumorigenesis (Sandberg et al. 2008; Mayr and Bartel 2009; Miles et al. 2016; Masamha et al. 2014; Chen et al. 2018b). APA factor expression is altered in a variety of cancer types and promotes tumorigenesis by regulating the expression of oncogenes (via loss of miRNA regulation) and tumor suppressors (via disruption of competing-endogenous RNA crosstalk) (Chen et al. 2018b; Mitra et al. 2018; Masamha et al. 2014; Li et al. 2015; Park et al. 2018). The relevance of APA in cancer was established with the discovery of a systemic increase in the usage of a proximal PAS leading to consistently shortened 3' UTRs of oncogenes such as Insulin-like growth factor 2 mRNA binding protein 1 (*IGF2BP1*), Ras-Related C3 Botulinum Toxin Substrate 1 (*RAC1*) and Cyclin D2 *(CCND2)* (Mayr and Bartel 2009; Chen et al. 2018b). Functional studies of the genes comprising the APA machinery have highlighted their relevance to tumor growth; for example, in glioblastoma, overexpression of the APA factor *NUDT21* (a repressor of proximal 3' UTR PAS usage) reduces tumor cell proliferation and inhibits tumor growth *in vivo* (Masamha et al. 2014). Subsequently, a number of pan-cancer analyses have utilized standard RNA-sequencing (RNA-seq) data to identify 3' UTR shortening and lengthening events across cancer types (Le Pera et al. 2015; Feng et al. 2017; Ye et al. 2018; Grassi et al. 2016; Xia et al. 2014). While these analyses have uncovered recurrent APA events across multiple tumor types, they also detected tumor type-specific events (Xue et al. 2018). Additionally, differential 3' UTR processing has been shown to drive tissue-specific gene expression (Lianoglou et al. 2013). However, there has been no in-depth single cancer analysis with a sufficiently large patient cohort to unravel disease-specific APA alterations. Furthermore, none of the pan-cancer studies have included PDA due to a lack of matched normal controls and therefore, the landscape of APA in PDA remains completely uncharacterized.

To determine the relevance of APA in PDA, we performed a comprehensive analysis of the changes in PAS usage using RNA-seq data from 148 PDA tumors from The Cancer Genome Atlas TCGA-PAAD (Pancreatic Adenocarcinoma) study and 184 normal pancreata from the Genotype-Tissue Expression (GTEx) project (The Cancer Genome Atlas et al. 2013; The GTEx Consortium 2015). We performed a systems level analysis to identify trends in APA, impacts on gene expression, and effects of miRNA regulation. Our in-depth analysis reveals APA as a recurrent, widespread mechanism underlying oncogenic gene expression changes through loss of tumor suppressive miRNA regulation in pancreatic cancer.

RESULTS

To analyze differences in APA profiles between tumor and normal samples, we selected 148 patients out of the total 178 PDA patients with aligned RNA-seq data from the TCGA-PAAD study. We excluded 30 patients in the cohort that did not have histologically observable PDA tumors (Raphael et al. 2017). Due to the paucity of RNA-seq data from matched normal tissues within the TCGA-PAAD study, we procured raw RNA-seq reads from 184 normal pancreata from the GTEx project. The library preparation and sequencing platform were identical for the TCGA-PAAD study and GTEx pancreata data (Raphael et al. 2017; The GTEx Consortium 2015), thereby minimizing potential batch effects. Several previous studies have successfully compared TCGA and GTEx gene expression data, noting minimal batch effects when processed in an identical manner (Zeng et al. 2019; Kosti et al. 2016; Aran et al. 2017). Therefore, these datasets were processed identically and analyzed for differences in APA in our downstream analyses (Supplemental Fig. S1). To allow a rigorous comparison between GTEx normal pancreas and TCGA-PAAD tumor samples, we aligned raw reads from the GTEx RNA-seq data as per the TCGA pipeline. We processed the tumor and normal aligned files to generate coverage files that were used to identify 3' UTR differences. We assessed the extent of differential batch effects by comparing the variation in expression of housekeeping genes between the two datasets (Eisenberg and Levanon 2003). We computed the median expression ($\log_2$(normalized counts)) of housekeeping genes from our coverage data and found a high correlation between the tumor and normal datasets (Pearson R=0.91, $p< 2 \times 10^{-16}$, Supplemental Fig. S2A), suggesting that the two datasets are comparable. The coverage data were used as an input for the DaPars (Dynamic Analysis of Alternative Polyadenylation from RNA-seq) algorithm (Xia et al. 2014). DaPars is a regression-based algorithm that performs de-novo identification of APA events between two conditions using standard RNA-seq data (Xia et al. 2014; Chen et al. 2018b; Masamha et al. 2014). DaPars generates a PDUI (Percentage Distal Usage Index) score for a given gene for every sample. The PDUI score quantifies the relative poly(A) site usage for that gene in the sample by computing the abundances of 3' UTR long and short forms. Genes favoring distal PAS usage (long 3' UTRs) have PDUI scores near 1, while genes favoring proximal PAS usage (short 3' UTRs) have PDUI scores near 0. The final output was a PDUI matrix containing 2573 unique genes as rows and tumor/normal sample in each column (total 148 tumor + 184 normal = 332 columns). To compare 3' UTR changes for a given gene between tumor and normal samples, the PDUI scores for the gene were averaged over tumor (MeanPDUI_T) and normal (MeanPDUI_N) samples. A change in the mean PDUI score

between tumor and normal samples for each gene (ΔPDUI= $MeanPDUI_T$ - $MeanPDUI_N$) was calculated and used as a measure of tumor-associated 3' UTR shortening or lengthening.

Integrative analysis of GTEx and TCGA-PAAD RNA-seq data identifies 3' UTR shortening events associated with PDA. To determine an appropriate ΔPDUI threshold to identify shortened/lengthened genes, we performed a permutation test (n=10000) and computed the adjusted p-values (p_{adj}) for ±0.05, ±0.1 and ±0.15 thresholds. 23.8% of genes showed p_{adj}>0.05 for a threshold of ±0.05, suggesting that this threshold can lead to multiple false positives. However, 0 genes showed p_{adj}>0.05 for the ±0.1 and ±0.15 thresholds (Supplemental Fig. S2B,C). Therefore, we chose ΔPDUI =±0.1 as a stringent threshold to identify shortened/lengthened genes with minimum false positives/negatives. To determine the extent of APA-mediated 3' UTR shortening and lengthening in PDA, we compared the PDUI scores for each gene between the tumor and normal samples (Fig. 1A,B). While the majority of genes do not undergo changes in APA, PDA patients are characterized by a greater number of significant 3' UTR shortening events (red dots, n=266) as compared to significant lengthening events (blue dots, n=186) (Fig. 1B). A higher number of 3' UTR shortening events compared to lengthening events in PDA is consistent with patterns observed in multiple pan-cancer analyses (Mayr and Bartel 2009; Xiang et al. 2018; Xia et al. 2014). The tumor-associated shortening and lengthening events were predominantly 100-300bp and 200-300bp in length, respectively (Fig. 1C). Amongst the genes found to have significantly shortened 3' UTR lengths were many known PDA growth-promoting genes, including *PAF1* (Polymerase Associated Factor 1), *FLNA* (Filamin-A), *ENO1* (α Enolase), *RALGDS* (Ral guanine nucleotide dissociation stimulator), *TRIP10* (Thyroid Hormone Receptor Interactor 10) and *ALDOA* (Aldolase A). *ALDOA* and *PAF1* have recently been described as oncogenes in PDA (Ji et al. 2016; Dey et al. 2014; Nimmakayala et al. 2018; Vaz et al. 2014), while *ENO1, RALGDS, TRIP10* and *FLNA* are known to mediate pancreatic cancer cell proliferation, survival and migration (Hsu et al. 2011; Zhou et al. 2011; Li et al. 2009; Capello et al. 2016; Chien and White 2003; Mihaljevic et al. 2010). We did not detect 3' UTR alterations in recurrently mutated PDA genes, reflecting the predominant role of APA in regulating gene expression rather than gene function. We visualized the 3' UTR profiles of these genes between TCGA and GTEx samples to confirm 3' UTR shortening (see *FLNA*, *PAF1* as examples, Fig. 1D).

PDA samples are often characterized by substantial stromal contamination (Maurer et al. 2019)**;** therefore, we sought to determine if significant APA events were present in the stroma or the

tumor epithelium. First, we determined for every significant gene hit in our analysis whether sample purity is correlated with the PDUI score. The measure of purity considered for each sample was the pathologist reviewed tumor cellularity score (Raphael et al. 2017). However, none of our significant gene hits showed a significant correlation (Pearson $R>0.3$, $p<0.05$) between PDUI score and tumor purity. We then analyzed PDUI changes in a subset of 69 high purity TCGA-PAAD tumor samples (Raphael et al. 2017) (>33% tumor content). 89% of gene hits from our original analysis showed up as significant hits in the high purity dataset, suggesting that the majority of the detected APA changes were not attributable to stromal contamination (Supplemental Fig. S3A,B)**.** We further addressed this concern by visualizing the 3' UTR profile of our candidate genes in an independent dataset containing RNA-seq information from 65 matched human PDA samples with micro-dissected tumor epithelium and stroma (Maurer et al. 2019; Maurer and Olive 2019). As an example, Fig. 1E shows the differential 3' UTR shortening of *FLNA* and *PAF1* in patient tumor epithelium (tumor cells) as compared to the matched stroma.

We validated the presence of alternative 3' UTR forms for several APA-regulated candidate genes by 3' RACE (rapid amplification of 3' ends) in 2 human pancreatic cancer cell lines (Suit2, MiaPaCa2) and primary patient samples (Fig. 1F,G). These genes included the previously described PDA growth-promoting genes, as well as the spermine/spermidine acetyltransferase *SAT1*, and PP2A subunit B isoform δ (*PPP2R2D*). SAT1 modulates cell migration and resistance in multiple tumor types, while PPP2R2D is a component of the tumor suppressive phosphatase PP2A (Vandenberg 2008; Seshacharyulu et al. 2013; Yu et al. 2018; Brett-Morris et al. 2014; Phanstiel 2018; Fahrmann et al. 2018). With the exception of *PPP2R2D*, which displayed significant 3' UTR lengthening and downregulation in tumors, all of the validated genes were significantly shortened and overexpressed in the TCGA-PAAD dataset. We detected 3' UTR short and long forms via 3' RACE. The short 3' UTR form for the majority of the shortened genes predominated over the long form (Fig. 1F,G). *ENO1* showed a single 3' UTR form suggesting that this is the predominant form in cancer cells. In contrast, *PPP2R2D* showed an increased proportion of the 3' UTR long form in PDA cell lines and patient samples as compared to the short form, suggesting greater use of the distal PAS for this putative tumor suppressive gene. For every candidate, we successfully identified PAS sites within its 3' UTR sequence that matched the expected position of proximal and distal PAS in the detected 3' RACE forms (Supplemental Fig. S3C). Therefore, a large-scale comparison of 3' UTR

alterations can identify tumor epithelium-specific changes from the TCGA and GTEx datasets, and these 3' UTR forms can be detected in cell models and patient samples.

3' UTR changes are widespread among PDA patients and enriched in PDA pathways.

To visualize the landscape of APA across PDA, we clustered patients (columns) based on change in PDUI score (tumor - normal mean; ΔPDUI) for 3' UTR altered genes (rows) (Fig. 2A). This analysis uncovered a subset of genes (n=68) that showed 3' UTR shortening (red) in >90% of patients, highlighting the widespread nature of APA across PDA. A smaller subset of 3' UTRs (n=26, bottom heatmap) was recurrently lengthened (blue) in the tumor cohort. Hierarchical clustering identified multiple patient subgroups characterized by 3' UTR alterations of specific gene sets (Subgroups 1-5). Subgroup 5 was enriched in shortened 3' UTRs and contained relatively few lengthening events. In contrast, Subgroup 1 displayed fewer 3' UTR shortening events and was enriched in 3' UTR lengthening. Subgroups 2-4 were characterized by shortening events in specific subsets of genes. These subgroups did not correlate with the mutational status of recurrently mutated PDA genes (*KRAS, CDKN2A, SMAD4, TP53*), nor did they associate with previously described PDA subtypes.

Pathway analysis of the significantly altered genes revealed enrichment for mRNA 3' end processing and splicing, as well as smooth muscle contraction and platelet activation. Similar pathways have been found by pan-cancer APA analyses, concordant with the presence of recurrent APA events across multiple cancer types (Xia et al. 2014; Lianoglou et al. 2013). However, we observed further enrichments in PDA-associated pathways, including protein metabolism, signaling by receptor tyrosine kinases, signaling by RHO GTPases, JAK-STAT signaling and cell-extracellular matrix interactions (Fig. 2B). Therefore, APA alterations may regulate the activity of PDA-promoting pathways.

3' UTR shortening identifies a poor prognostic cohort in PDA patients.

Next, we asked whether APA events added additional prognostic information to PDA patient outcomes above the usual demographic and clinical factors: age, race, sex, stage, grade and surgical outcome. We selected genes with significant 3' UTR alterations and univariate prognostic value, defining prognostic classes based on multivariate clustering (Fig. 3A). This segregated patients into three cohorts based on their 3' UTR patterns (long=blue; short=red). Cohort A was predominantly associated with proximal PAS usage of genes from Groups 1 and 3, while cohort C was associated with distal PAS usage of the same genes. For Group 2 genes,

distal PAS usage was predominant in cohort A while proximal PAS usage was predominant in cohort C. Neither patient cohort correlated with any of the known PDA tumor subtypes. Cohorts A and C displayed significant differences in overall survival, with patients in cohort C living significantly longer than those in cohort A (p=0.003) (Fig. 3B). Therefore, patterns of APA can be used as an independent prognostic indicator in PDA.

Heterogeneity of proximal PAS usage of metabolic genes in PDA patients.

Processes generating genetic and epigenetic heterogeneity can drive tumor evolution (Hinohara and Polyak 2019; Easwaran et al. 2014; McGranahan and Swanton 2017). We hypothesized that APA could represent such a process, creating a diverse set of 3' UTR forms and allowing cancer cells to select for those that promote their survival and propagation. To examine this heterogeneity, we compared the variance of proximal PAS usage across patients in any given gene between tumor and normal samples. *ALDOA* is shown as an example gene that exhibited a tight distribution of PAS usage across normal as well as patient tumors (Fig. 4A). The left shift of the tumor sample mean score represents an increased proximal PAS usage signifying the expected shortening of the *ALDOA* 3' UTR. However, for *FLNA*, while the normal samples had a tight distribution, PDA patients showed greater heterogeneity in PAS usage (Fig. 4B). An analysis of heterogeneity in PAS usage for all genes revealed that while the majority of genes did not show a significant change between normal and tumor conditions, 89 genes showed greater heterogeneity in tumor (orange) samples and only 8 genes showed greater heterogeneity in normal (purple) samples (Fig. 4C). This heterogeneity was not due to intrinsic differences between the TCGA and GTEx datasets because none of the 215 housekeeping genes in the dataset showed differences in heterogeneity in the extent of proximal PAS usage (Eisenberg and Levanon 2013; Zhu et al. 2008). The subset of 89 genes was enriched in metabolic genes, specifically amino acid transporters and purine metabolism. Increased heterogeneity of PAS usage in PDA patients suggests a possible role of PAS usage plasticity in promoting cancer cell survival and progression.

APA drives altered protein expression in PDA. To determine whether the identified APA events drive altered gene expression in PDA, we computed differential gene expression between normal (GTEx) and tumor (TCGA-PAAD) tissues. This allowed association studies between specific APA events and changes in gene expression. Among 3' UTR shortened genes, 76 were significantly upregulated, while 50 genes were significantly downregulated in tumors (Fig. 5A,B). Increased gene expression in the subset of 76 genes conforms to the

expectation that 3' UTR shortened genes can escape miRNA regulation leading to increased gene expression (Mayr et al. 2007; Lee and Dutta 2007; Mayr and Bartel 2009). However, the association of 3' UTR shortened genes with upregulation was not statistically significant (Fisher's exact test, p=0.09). 3' UTR lengthened genes showed a similar number of significantly upregulated (n=42) and significantly downregulated (n=41) genes, consistent with pan-cancer analyses, and most likely reflective of positive and negative regulation by RNA-binding proteins (Pereira et al. 2017; Matoulkova et al. 2012; Chen et al. 2018a).To experimentally validate the relationship between APA and protein expression, we performed luciferase reporter assays in MiaPaCa2 cells, comparing protein expression driven by short and long 3' UTRs (Fig. 5C). We focused on the candidate oncogenes and tumor suppressors validated by 3' RACE and that showed significant association between 3' UTR changes and gene expression in tumors. These candidates included *ALDOA, FLNA, PAF1, TRIP10, ENO1*, *SAT1* (shortened and upregulated in tumors) and *PPP2R2D* (lengthened and downregulated in tumors). We also included *RALGDS* which is shortened but does not show altered expression in tumors. We cloned the short and long 3' UTRs of each gene (estimated via 3' RACE) downstream of a *Renilla* luciferase reporter and measured luminescence as a readout of protein expression (Fig. 5C). To ensure that the long 3' UTR form for each reporter gene remained intact (*i.e.*, did not undergo APA-mediated shortening upon transfection into cells), we mutated their functional proximal PAS. For all genes tested except *ENO1* and *RALGDS*, the short 3' UTR form showed significantly increased luminescence compared to the long 3' UTR form (Fig. 5D). As predicted, the 3' UTR short and long forms of *RALGDS* showed similar expression. In contrast to our expectations, the short form of *ENO1* showed decreased protein expression suggesting that 3' UTR shortening is not the sole mechanism regulating protein abundance of *ENO1* in PDA. To further demonstrate that the expression changes driven by the short and long 3' UTR forms are governed by the sequence content and not simply a function of 3' UTR length, we cloned the reverse complement of the long 3' UTR segment of *PAF1* downstream of its short 3' UTR. The proximal PAS was mutated to prevent APA-mediated shortening of this control construct (Supplemental Fig. 4A). As expected, this construct showed similar luminescence as the short 3' UTR form, suggesting that the observed expression differences are primarily a function of sequence content within the long 3' UTR (Supplemental Fig. 4B). These findings reinforce the observation that gene regulation is 3' UTR sequence-dependent and that shorter 3' UTRs do not always increase protein expression (Mayr and Bartel 2009). Overall, the above results demonstrate that APA-mediated 3' UTR alterations can regulate the protein expression of growth-promoting genes in PDA cells.

We next sought to determine the mechanism underlying the 3' UTR-mediated gene regulation of the PDA oncogene *ALDOA*. Given that miRNAs primarily destabilize their target mRNA and that *ALDOA* undergoes 3' UTR shortening and upregulation, we searched the *ALDOA* 3' UTR for putative miRNA binding sites that would be lost upon PDA-associated shortening (Fig. 5E). We identified the tumor suppressive miRNA miR-122 within this lost region; miR-122 is expressed in PDA cell lines (Tsai et al. 2009; Zhang et al. 2009). Mutation of the miR-122 site within the long 3' UTR of *ALDOA* significantly restored protein expression (Fig. 5F). Therefore, altered APA can regulate oncogene expression in PDA through modulation of available regulatory miRNA binding sites.

APA-mediated loss of tumor suppressive miRNA binding sites is associated with poor patient outcome. To assess global patterns of APA-mediated miRNA binding site loss we searched for highly conserved miRNA binding sites (conserved across human, mouse, rat, dog and chicken) within the lost 3' UTRs of all shortened genes. This analysis revealed that 42% of genes lost at least one highly conserved miRNA binding site (Fig. 6A), suggesting that alteration of the miRNA binding site repertoire is a common mode of APA-mediated regulation. Next, we sought to determine if any miRNA families were preferentially lost in shortened 3' UTRs of PDA patients. We computed an index for repression for each miRNA family as a function of the miRNA site context scores (obtained from TargetScan) and the abundance of the 3' UTR form containing that site. This index was then compared between PDA patients and normal controls to yield a Z-score. A lower Z-score for a miRNA family reflects preferential loss of its binding sites due to 3' UTR shortening. We focused on the top 8 miRNAs as after the 8th miRNA, all subsequent significantly lost miRNAs had similar z-scores (near -1) and all 8 are expressed in pancreatic cancer cell lines (Zhang et al. 2009). 6 of these top 8 miRNAs have been implicated as tumor suppressors in PDA, including miR-329 and miR-133a (Dangi-Garimella et al. 2011; Wang et al. 2019; Qin et al. 2014; Wang et al. 2016; Baradaran et al. 2019) (Fig. 6B). These results suggest that APA regulates oncogenic gene expression through preferential loss of tumor suppressive miRNA binding sites and may therefore confer a selective advantage to the cell.

Next, we determined whether loss of specific miRNA sites associated with 3' UTR alterations is associated with patient outcome. We quantified loss of highly conserved miRNA binding sites for each patient as a function of the extent of proximal PAS usage in all genes that lost those miRNA sites (see Methods). Clustering in the miRNA feature space revealed 3 patient groups

(Fig. 6C) with significant differences in overall survival (p=0.012 between Clusters 1 and 3; Fig. 6D). We also performed the analysis of deviance test of the nested Cox regression model: clinical variables versus clinical + miRNA clusters. We found that addition of miRNA clusters significantly improved the model. In terms of magnitude of effect, the hazard ratios associated with the miRNA clusters (Cluster 1/Cluster 3 as reference) were HR=0.59 and HR=0.44. For context, the strongest significant clinical effect is HR=0.52 for R0 surgical status. This suggests the miRNA-usage based modeling is at least as strong as clinical variables. The miRNAs most significantly associated with the patient clusters included miR-133a, miR-124, miR-421, miR-143 and miR-505. Binding sites for each miRNA were preferentially lost from Cluster 1 as compared with Cluster 3, suggesting that loss of these regulatory sites correlates with poor survival of PDA patients (Fig. 6E). Indeed, miR-133a, miR-124 and miR-143 are known tumor suppressors in PDA, again supporting the role of APA in selective loss of tumor suppressive miRNA binding sites (Hu et al. 2012; Qin et al. 2014; Schultz et al. 2014; Wu et al. 2018; Pham et al. 2013; Kojima et al. 2012; Kent et al. 2010).

The APA-regulated gene *CSNK1A1* is required for proliferation and clonogenic growth of PDA cells.

Our analyses revealed APA-mediated regulatory changes in genes known to promote PDA pathogenesis. We hypothesized that our altered gene list may also contain growth-promoting genes not previously implicated in PDA biology, and therefore new therapeutic targets. We focused on the subset of druggable genes that were significantly shortened and upregulated in PDA. This analysis identified *CSNK1A1*, the gene encoding the serine/threonine kinase casein kinase 1 alpha (CSNK1A1, also known as CK1alpha or CK1a). CSNK1A1 regulates the Wnt/β-catenin signaling pathway and has dual functions in cell cycle progression and cell division (Schittek and Sinnberg 2014; Knippschild et al. 2005; Cai et al. 2018). CSNK1A1 is known to influence tumor progression; however, its role as a tumor suppressor or oncogene is tumor type-dependent (Cai et al. 2018; Schittek and Sinnberg 2014; Lantermann et al. 2015; Järås et al. 2014) and CSNK1A1 has no known roles in PDA. *CSNK1A1* has very low gene expression in normal pancreas but is overexpressed in PDA (Jiang et al. 2018). We found that *CSNK1A1* shows significantly higher expression in the PDA epithelium as compared to precursor lesions (premalignant pancreatic intraepithelial neoplasia (PanIN) (Fig. 7A) and intraductal papillary mucinous neoplasia (IPMN)). We found no significant difference in *CSNK1A1* expression in the stroma between PDA and precursor lesions. 3' RACE showed that *CSNK1A1* has both the short

and long 3' UTR forms in PDA cells as predicted by our computational analysis (Supplemental Fig. S5A).

To provide genetic evidence for the role of CSNK1A1 in PDA cell growth, we knocked down *CSNK1A1* in Suit2 and MiaPaCa2 cells with 3 short hairpin RNAs (shRNA) (Fig. 7B, Supplemental Fig. S5B). *CSNK1A1* knockdown decreased both cell proliferation and clonogenic growth of PDA cells (Fig. 7C-E, Supplemental Fig. S5C,D), with Suit2 cells showing increased sensitivity to CSNK1A1 loss. The strongest phenotypic effects were associated with the most efficient knockdown (shRNA 3) in both cell lines. We then investigated the potential of CSNK1A1 as a pharmacological target in PDA biology with the widely used small molecule inhibitor D4476 (Rena et al. 2004; Lantermann et al. 2015; Jiang et al. 2018). In concordance with the genetic evidence, while MiaPaCa2 and Suit2 cells were both sensitive to D4476 treatment, Suit2 cells displayed a 10-fold lower IC50 (Fig. 7F). Both cell lines also showed dose-dependent decreases in cell proliferation (Fig. 7G, Supplemental Fig. S5E) and clonogenic growth in the presence of the inhibitor (Fig. 7H,I, Supplemental Fig. S5F). Therefore, we identify CSNK1A1 as a putative drug target in PDA and reveal the potential of cancer-specific APA analyses to identify mechanisms of altered gene expression driving cancer pathogenesis.

DISCUSSION

Dysregulated gene expression is a cardinal feature of cancer (Yaffe 2019). However, how gene expression is altered in cancer and whether the processes driving this dysregulation can be targeted therapeutically are areas of active investigation. APA has recently been identified as a candidate driver of gene expression dysregulation. APA factors frequently show aberrant expression in cancer, modulate the expression of known oncogenes and tumor suppressors, and knockdown studies have highlighted their relevance to the cancer phenotype (Chu et al. 2019; Tan et al. 2018; Chen et al. 2018b; Miles et al. 2016; Mitra et al. 2018; Masamha et al. 2014). Whole-genome CRISPR and shRNA screens have also revealed the requirement for several APA factors in pancreatic cancer cell growth (www.depmap.org). Global analyses have revealed widespread 3' UTR changes across multiple cancer types, uncovering recurrent alterations common across the cancer spectrum (Grassi et al. 2016; Ye et al. 2018; Feng et al. 2017; Xia et al. 2014). Recent findings suggest that while some APA events are widely shared across cancers, many are tumor type-specific (Xue et al. 2018). Despite this observation, there have been few attempts to study APA in a single tumor type with sufficient power to identify tumor-specific alterations and vulnerabilities.

To our knowledge, this study represents the first global, in-depth, single cancer view of APA, and the first examination of APA in PDA clinical samples. The only previous study of APA in PDA showed gemcitabine-induced 3' UTR shortening of the transcription factor ZEB1 in the context of drug resistance (Passacantilli et al. 2017). Previous APA analyses combined multiple tumor types and used tumor-adjacent tissue as a "normal" control. However, matched tumor-adjacent normal tissues are known to represent a state that significantly differs from healthy, normal tissues and may therefore miss critical APA events (Aran et al. 2017). Furthermore, there are insufficient numbers of tumor-adjacent pancreatic samples within TCGA for a statistically stringent analysis. Therefore, we attempted to address these issues by using normal pancreas RNA-seq information from the GTEx project. A limitation of comparing independently collected datasets is the inherent disparity between them (Lappalainen et al. 2013). We attempted to rectify this by: a) confirming that the two datasets underwent identical library preparation methods on the same type of sequencing platform; b) following identical data processing pipelines from the raw sequencing data to generate the coverage data; c) validating our top hits in an independent micro-dissected dataset. Consistent with previous publications comparing TCGA and GTEx datasets, we compared the expression of housekeeping genes between the two datasets and observed minimal differences. As batch effects cannot be

completely ruled out, we performed experimental validation of several candidate APA regulated genes, including *PAF1* and *ALDOA*, highlighting the robustness of our approach and relevance of our findings to PDA biology. Furthermore, this approach will allow the analysis of APA in other tumor types for which little tumor-adjacent material is present in TCGA.

Multiple insights from our analyses are noteworthy. We find that APA events are recurrent and widespread across PDA patients. For example, 68 genes were shortened and 28 genes were lengthened in greater than 90% of the patient cohort. This supports the conjecture that APA dysregulation is a frequent event in PDA. In support of this hypothesis, we find that several APA factors are highly expressed in PDA, including *CSTF2* (Supplemental Fig. S6). CSTF2 has previously been implicated as a promoter of lung and bladder cancer, through the regulation of *ERBB2* and *RAC1* 3' UTRs, respectively (Mitra et al. 2018; Chen et al. 2018b). We find frequent 3' UTR alterations in several PDA-relevant genes whose mechanisms of regulation were previously unknown, including *PAF1*, *ALDOA* and *FLNA*. Many of the shortened 3' UTRs showed increased gene expression, providing the first collection of 3' UTR alterations that correlate with gene expression changes in PDA. We were able to functionally validate these through luciferase reporter assays, highlighting the robustness of our analysis. Consistent with pan-cancer APA analyses, we find enrichment for pathways such as smooth muscle contraction and mRNA 3'-end processing (Lianoglou et al. 2013; Chen et al. 2018a; Xia et al. 2014). However, we also find enrichment for pathways and processes implicated in PDA biology, including protein metabolism, receptor tyrosine kinase signaling and signaling by RHO GTPases. Indeed, the link between 3' UTR alterations and cancer metabolism has been identified in previous pan-cancer APA analyses (Xia et al. 2014). We also find an unexpected enrichment for loss of binding sites for tumor-suppressive miRNAs in frequently lost 3' UTR regions. Therefore, we propose that APA is an underappreciated mechanism of gene dysregulation in PDA, driving the expression of growth-promoting genes through disruption of miRNA-mediated regulation.

The extent of heterogeneity in proximal PAS usage across cancer patients has been largely overlooked in previous pan-cancer APA analyses**.** We found little heterogeneity in the extent of 3' UTR proximal site usage in most genes (including housekeeping genes) in both normal and PDA samples, again providing evidence for minimal batch effects. However, PDA patients showed substantial heterogeneity in the extent to which their metabolic genes used the proximal PAS. This metabolic plasticity in turn could serve as a mechanism to deal with the fluctuating

metabolic demands of cancer cells. These data support the possibility that APA may drive deregulation of cancer metabolism and tumor evolution by allowing for PAS choice plasticity of critical metabolic genes in PDA.

Several studies have demonstrated the power of APA analysis to improve expression-based prognostic markers. We report the first subset of 3' UTR alterations that act as an independent prognostic indicator of PDA outcome. While several of the genes in this set are known regulators of tumorigenesis, including *SAT1*, many have not been implicated in PDA biology and may represent new mediators of cancer phenotypes. The lost miRNA sites are enriched for tumor-suppressive miRNA families. In particular, we observed that patients who retain binding sites for a subset of 5 miRNAs survive longer than patients who lose them. This uncovers the prognostic role for a novel subset of miRNA mediators in PDA.

Our in-depth analysis of APA in PDA revealed a critical role for the druggable target CSNK1A1 in PDA cell growth and survival. While CSNK1A1 regulates Wnt signaling and the *TP53* pathway, mediators of PDA progression, the relevance of CSNK1A1 to PDA was previously unknown (Jiang et al. 2018; Järås et al. 2014; Lantermann et al. 2015; Cai et al. 2018). Furthermore, the mechanisms of regulation of CSNK1A1 in cancer are not well understood, although promoter methylation in melanoma has been reported (Sinnberg et al. 2010). Two *CSNK1A1* isoforms have been detected in HeLa cells, with the shorter isoform being generated from the use of an alternative PAS (Yong et al. 2000). We show that *CSNK1A1* exhibits increased expression in PDA samples as compared to precursors, and that pharmacological and genetic blockade of CSNK1A1 attenuates PDA cell proliferation and clonogenic growth. Therefore, our single-cancer approach can identify APA-regulated, disease-specific vulnerabilities.

Our computational analysis and experimental validation have revealed unexpected mediators of PDA biology and broadened our understanding of the regulatory role of 3' UTR sequence space in cancer. This comprehensive analysis reveals the scope of previously uncharacterized APA events in regulating functionally relevant PDA genes, improving patient prognosis and driving tumor evolution. We propose that the landscape of 3' UTR alterations in PDA represents a novel avenue to better understand PDA progression and identify new drug targets.

MATERIALS AND METHODS

Data collection and preprocessing

Our study focused on PDA tumors consistent with the histology of PDA (n=148). All raw RNA-seq data used in this study were downloaded via NCBI dbGaP after our request for controlled-access data was processed. This included 184 normal pancreas SRA files from GTEx (dbGaP accession phs000424.v8.p2) and 148 BAM files within the TCGA-PAAD cohort (https://portal.gdc.cancer.gov/). GTEx SRA files were aligned exactly according to the TCGA RNA-seq alignment pipeline using GENCODE.v22 annotations. The bedGraph files were generated using BEDToolsv2.26 (Quinlan and Hall 2010) and were supplied as input to the DaPars algorithm.

DaPars analysis

The bedGraph coverage files were processed using DaPars (Python 2.7.13) for *de novo* identification of differences in 3' UTR between tumor and normal samples. The output of DaPars is a matrix of PDUI scores for every sample (columns) for any given gene (rows). Each cell represented a PDUI score for a gene corresponding to the tumor or normal sample. The PDUI score for a given gene represents the percentage of distal PAS usage in the sample. A higher PDUI score represents greater usage of the distal PAS site. In order to compare 3' UTR changes for a given gene between tumor and normal samples, the PDUI scores for the gene was averaged over tumor samples ($MeanPDUI_T$) and normal ($MeanPDUI_N$) samples. A change in the mean PDUI score between tumor and normal samples for each gene ($\Delta PDUI = MeanPDUI_T - MeanPDUI_N$) was computed as a measure of 3' UTR differences. The significance of this difference was assessed by the algorithm using Fisher's exact test, which was further adjusted using Benjamini-Hochberg (BH) procedure to control the false discovery rate using 0.05 as a threshold to select significant hits. The final output of our analysis after eliminating redundant transcripts (based on lowest FDR) and selecting for protein-coding transcripts was a matrix containing 2573 unique genes as rows and tumor/normal sample in each column (total 148 tumor + 184 normal = 332 columns). Given that our samples are not matched, we did not generate a $\Delta PDUI$ value for a given gene for every sample, rather we have a unique $\Delta PDUI$ value for every outputted gene. A similar analysis was performed with a subset of 69 high purity PDA tumor samples (Raphael et al. 2017).

Bioinformatics analyses and statistical methods

Analysis of heterogeneity. The variance in PDUI scores across tumor samples (Var(Tumor)) as well as normal samples (Var(Normal)) was computed for every gene as a measure of its heterogeneity in PAS site usage across samples. The difference in variance/heterogeneity between the two datasets (Var(Normal)-Var(Tumor)) was plotted (R version 3.6.0, R Core Team 2014). The significance of the difference for each gene was assessed using F test of variances.

Heatmap analysis. A heatmap representing the extent of 3' UTR alterations across PDA patients was generated (R version 3.6.0). Given that we do not have a ΔPDUI value for each patient, we computed an estimate of ΔPDUI associated with each patient for any given gene, using the following approach. For each significant gene hit (|ΔPDUI|>0.1, row in heatmap), the mean GTEx PDUI score was subtracted from the PDUI score for each TCGA PDA patient to obtain a measure of $\Delta PDUI_{patient}$ (change in 3' UTR length for that gene for each patient). We implemented unsupervised hierarchical clustering using Ward's minimum variance method, to minimize the inter-cluster Euclidean distances. Rows were similarly clustered to yield subsets of genes undergoing a higher degree of 3' UTR shortening (red) or lengthening (blue). 5 distinct subgroups are presented to visualize the patterns of widespread 3' UTR shortening among patients. The mutational status of commonly altered PDA genes and PDA subtype for each TCGA patient was highlighted (Raphael et al. 2017).

Survival analysis. We first fit a complex clinical model including diagnosis age, stage, grade, residual tumor, sex and race. Residuals from this model reflect signal not explained by the standard clinical subspace. PDUI scores associated with the residuals were then screened to identify a multivariate subspace to study. We selected 20 features (genes) to study based on p-value order. Using repeated random starts, we selected K=3 *k*-means clustering based on the elbow heuristic to define 3 prognosis groups based on the within/between sum of squares criterion. The prognostic value of this classification is described by standard Kaplan-Meier plot and the log-rank test. We determined that 85% of random re-starts led to statistically significant log-rank tests for K=3 suggesting that significant additional prognostic information in the PDUI subspace above the clinical data was stable as opposed to stochastic clustering.

Percentage of lost miRNA sites. Highly conserved miRNA binding sites and their genomic positions were downloaded from TargetScanHuman 7.2. This list, along with DaPars prediction of genomic coordinates of lost 3' UTRs was used to plot the number of genes that lose at least 1 highly conserved miRNA binding site.

miRNA families preferentially associated with lost sites. In order to determine miRNAs associated with sites enriched in lost 3' UTRs, miRNA target predictions and the cumulative weighted context++ scores (CWCS) were downloaded from TargetScanHuman 7.2. CWCS estimates the predicted cumulative repression for a miRNA at the site. The lost miRNA binding sites in the shortened 3' UTRs of PDA patients were inferred from DaPars predictions. A weighted target site score was computed as the sum over all genes with shortened 3' UTRs in tumor, with the CWCS of each target site for the miRNA multiplied by the normalized abundance of the gene's 3' UTR form in which the predicted target site was present. The fold-change (f) of the sum of weighted target site scores in lost 3' UTR regions for PDA tumor over normal was calculated (f=score in tumor/score in normal). The labels of the miRNA target sites were permuted to assess the significance of the fold-change. 1000 such randomizations were performed and the mean (m) and standard deviation (s) of the fold changes across the randomized data sets was computed. The significance of the fold change was computed in form of the Z-score defined as (f-m)/s. A lower Z-score indicates that the loss in miRNA binding sites is higher than that expected by chance.

miRNA prognostic signature. We quantified the impact of APA-based loss of miRNA binding as follows:

$$X_{m,i} = \Sigma_g \, (1\text{-}PDUI_{i,g}) \times A_{g,m}$$

where $A_{g,m}$ is an indicator function that the short versus long 3' UTR of the gene g contains the binding site for miRNA m, the impact to the i^{th} person is $X_{m,i}$. We used Sure Independence Screening (SIS) to search through all affected miRNAs and identify features that were associated with survival univariately (Fan and Lv 2008). To study the multivariate effect, we reorganized cases using the euclidean distance between SIS selected features, visualized with t-SNE, and defined clusters with model-based Gaussian clustering using the BIC criterion to select cluster number. Survival differences were tested across all groups by the log-rank test and were visualized by Kaplan-Meier estimate. We performed the analysis of deviance test of the nested Cox regression model: clinical variables versus clinical variables + miRNA clusters which was statistically significant (p=0.02) suggesting that addition of miRNA clusters improved the model. The pattern of loss of miRNA binding sites across patient clusters were visualized for a subset of miRNAs in a heatmap.

Experimental methods

Cell lines and general reagents.

MiaPaCa2 and HEK293 cells were purchased from ATCC and cultured in DMEM media (Cat# MT 10-013-CV, Corning) and 10% fetal bovine serum. Suit2 cells were obtained from Dr. David Tuveson (Cold Spring Harbor Laboratory). Cell lines were periodically verified to be mycoplasma free using the Mycoalert kit (Cat# LT07-701, Lonza). All transfections were carried out using Lipofectamine 3000 (Cat# L3000008, Thermo Fisher Scientific) as per manufacturers protocol.

3' RACE assays.

cDNA was generated from 1µg RNA from MiaPaCa2 as well as Suit2 cell lines using SuperScript II Reverse Transcriptase (Cat# 18064022, Thermo Fisher Scientific) using the primer P: 5'- GACTCGAGTCGACATCGATTTTTTTTTTTTTTTT-3'. To PCR amplify the 3' UTR forms of candidate genes, a gene specific forward primer spanning the stop codon of the gene was used in conjunction with a reverse primer P': 5'- GACTCGAGTCGACATCG-3' targeting the adapter region introduced by primer P. The PCR mixture was run on a 1.5% agarose gel and visualized using the Chemidoc imaging system followed by analysis with Image Lab software (Version 6.0.0, Bio-Rad). An identical cDNA generation and PCR procedure was followed for RNA extracted from PDA patient tumor samples. RNA from PDA patient samples were obtained from Roswell Park Pathology Shared Resource. Approval of biospecimen use was granted by the Roswell Park IRB.

Luciferase reporter assays.

MiaPaCa2 cells were seeded at ~10000 cells per well in a 96-well white plate (Cat# 07-200-628, Fisher Scientific). 3 technical replicates were plated for each condition. The cells were transfected the next day at ~ 60% confluency with 200ng of *Renilla* luciferase reporter plasmid (pIS1 containing the 3' UTR region of interest) and 2ng of firefly luciferase reporter control plasmid pIS0 per well. In cases where the 3' UTR lengths between the short and long form were significantly different, we ensured that equal molar amounts of the 3' UTR constructs were transfected. Luciferase readings were measured 24h post-transfection with the Dual luciferase reporter assay system (Cat# E1910, Promega) using the Synergy H1 plate reader. The *Renilla* reporter reading was normalized to its corresponding firefly reading in every well to control for transfection efficiency.

Statistical analyses.

All experimental findings presented were replicated in three or more independent experiments. Comparisons between two groups were performed using unpaired *t*-test with Welch's correction in Graph Pad Prism 8. In general, $p < 0.05$ was considered significant, and the determined p values are provided in the figure legends. Asterisks in graphs denote statistically significant differences as described in figure legends.

SOFTWARE AVAILABILITY

The code to pre-process RNA-seq data as well as the R code for all analyses is provided as Supplemental Code and is hosted in GitHub (github.com/feiginlab/APA_PDA).

ACKNOWLEDGEMENTS

This work was supported by NCI grants P30 CA016056 and R25 CA181003, an award from the Roswell Park Alliance Foundation to MEF, DoD grant OC170368 to KHE, and scholarship and support to AAA from Prince Sattam bin Abdulaziz University in Saudi Arabia, Saudi Arabian Cultural Mission in U.S. and the Office of International Collaborations in Oncology at Roswell Park Comprehensive Cancer Center. We thank the Roswell Park Gene Modulation core, Pathology Shared Resource, Genomics Shared Resource and the Small Molecule Screening Shared Resource for their assistance. We thank the members of the Feigin Lab, the Roswell Park Department of Pharmacology and Therapeutics, and the Science Twitter community for their helpful comments on the manuscript.

AUTHOR CONTRIBUTIONS

SV, MEF wrote the manuscript. MEF supervised the study. SV performed the DaPars analysis. SV, AAT, JRS and AAA performed biological experiments. SV, KHE, HCM, KPO contributed to data analysis. KHE developed prognostic signatures.

DISCLOSURE DECLARATION

The authors declare no competing financial interests.

687 **FIGURE LEGENDS**

688 **Figure 1. Integrative analysis of RNA-seq data identifies 3'-UTR alterations associated**
689 **with PDA.** (A) A plot of PDUI score of each gene in human tumor and normal samples. Dashed
690 lines represent 0.1 cutoffs. Blue dots represent 3'-UTR lengthened genes while red dots
691 represent 3'-UTR shortened genes. (B) A volcano plot denoting 3'-UTR shortened (red) and
692 lengthened (blue) gene hits (FDR<0.01) whose $|\Delta PDUI| > 0.1$. (C) A plot showing the number of
693 base pairs lost/gained by 3'-UTR altered genes. (D) UCSC Genome Browser plot depicting the
694 3'-UTR RNA-seq density profile of two 3'-UTR shortened genes (*FLNA* and *PAF1*) to highlight
695 the coverage differences between tumor (orange) and normal (purple) patient samples. (E)
696 UCSC Genome Browser plot highlighting the 3'-UTR profile differences between *FLNA* and
697 *PAF1* in a micro-dissected dataset in patient tumor (red) and stroma (blue). (F) 3'-RACE of
698 altered PDA-associated genes in MiaPaCa2 and Suit2 cells (representative images, n=3).
699 Approximate length of the 3'-UTR form is denoted beside each band. (G) 3'-RACE of select
700 genes in primary patient samples (P1, P2, P3).
701
702 **Figure 2. 3'-UTR changes are widespread among PDA patients and enriched in PDA**
703 **pathways.** (A) The heatmap shows genes (rows) undergoing 3'-UTR shortening (red) or
704 lengthening (blue) in each patient tumor (columns) compared to median score in normal
705 pancreas for that gene. The profile of *KRAS, CDKN2A, TP53, SMAD4* mutations as well as
706 tumor subtype is shown in the context of distinct APA-derived patient subgroups. (B)
707 Significantly enriched (FDR<0.05) reactome pathways associated with 3'-UTR altered genes.
708
709 **Figure 3. APA events identify a poor prognostic cohort in PDA patients.** (A) Patients were
710 clustered based on 3'-UTR short (red) and long forms (blue) of 3'-UTR altered genes (clustered
711 into gene groups 1,2,3) and segregated into patient cohort A (blue), patient cohort B (black) and
712 patient cohort C (green). (B) Kaplan-Meier survival plot for patient cohort A (blue), patient cohort
713 B (black) and patient cohort C (green) (*p<0.05).
714
715 **Figure 4. PDA patients show substantial heterogeneity in the extent of proximal PAS**
716 **usage of metabolic genes.** (A) Example of a 3'-UTR shortened gene (*ALDOA*) that has a tight
717 distribution of its proximal PAS usage in normal pancreas (purple) as well as PDA patients
718 (orange). (B) A 3'-UTR shortened gene (*FLNA*) that has a tight distribution in normal pancreas
719 (purple); however, the extent of proximal PAS usage varies greatly across PDA patients
720 (orange). (C) Plot of variance in PDUI for all genes between tumor and normal. Purple dots

represent genes with high variance in normal samples while orange dots represent genes with high variance in tumor samples. Dashed lines represent 0.015 and –0.015 cutoffs.

Figure 5. APA drives altered protein expression in PDA. (A) Log fold change in gene expression is plotted against ΔPDUI for 3'-UTR altered genes. Overexpressed genes (red dots) and underexpressed genes (blue dots) on the left represent 3'-UTR shortened hits while those to the right represent 3'-UTR lengthened hits. (B) Quantification of 3'-UTR altered genes that are overexpressed (red) or underexpressed (blue) in PDA tumors. (C) Schematic illustrating the luciferase reporter constructs. (D) Normalized fold expression change of the luciferase reporter (short 3'-UTRs / long-3'UTRs) for the selected list of 3'-UTR altered genes (n=3). The long 3'-UTR expression for each gene is normalized to 1. Each whisker plot denotes the median as the center line and the minimum and maximum values as the whiskers (*p<0.05, **p<0.01,***p<0.005, ****p<0.001). (E) Schematic showing the *ALDOA* 3'-UTR with positions of conserved miRNA sites as well as the miRNA mutant construct used. (F) Fold expression change of miRNA mutant construct compared to the PAS mutant in luciferase assays (n=3). The PAS mutant expression is normalized to 1.

Figure 6. APA-mediated loss of tumor suppressive miRNA binding sites is associated with poor patient outcome. (A) Number of genes that lose highly conserved miRNA binding sites due to 3'-UTR shortening. The percentage of genes that lose at least 1 miRNA binding site is indicated above the bracket. (B) Highly conserved miRNA families were plotted against their Z-score, an index of the lost binding sites where a more negative Z-score indicates more significant binding site loss. (C) t-SNE plot depicting TCGA patient clusters in the highly conserved miRNA feature space. (D) Kaplan-Meier survival plot for the 3 patient clusters identified in (C) (*p<0.05 for Cluster 1 to Cluster 3 comparison). (E) Heatmap depicting the association of miRNA binding site loss (miR score) with patient clusters.

Figure 7. CSNK1A1 is required for cell proliferation and is a putative drug target in PDA. (A) A plot showing *CSNK1A1* gene expression (in transcripts per million) in PDA (red) as compared to PanIN lesions (green) in the epithelium and stroma from micro-dissected samples (****p<0.001). (B) A representative blot confirming CSNK1A1 knockdown in Suit2 cells with a non-targeting control shRNA (Con shRNA) or with one of three different shRNAs targeting *CSNK1A1* (n=3). ACTB (also known as actin beta) is shown as a loading control. (C) Cell proliferation of Suit2 control and CSNK1A1 knockdown cells (n=3, ***p<0.005). (D) Clonogenic

growth assay of control and CSNK1A1 knockdown cells (n=3). (E) Quantification shows the number of colonies in (D) (n=3, ****p<0.001). (F) Dose-response of MiaPaCa2 (purple) and Suit2 (red) cell lines to the CSNK1A1 small molecule inhibitor, D4476 (n=3). (G) Cell proliferation of Suit2 cells treated with indicated doses of D4476 (n=3, ****p<0.001). (H) Clonogenic growth assay of Suit2 cells treated with indicated drug doses. (I) Quantification shows the number of colonies in (H) (***p<0.005, ****p<0.001).

REFERENCES

Aran D, Camarda R, Odegaard J, Paik H, Oskotsky B, Krings G, Goga A, Sirota M, Butte AJ. 2017. Comprehensive analysis of normal adjacent to tumor transcriptomes. *Nat Commun* **8**: 1077.

Bailey P, Chang DK, Nones K, Johns AL, Patch A-M, Gingras M-C, Miller DK, Christ AN, Bruxner TJC, Quinn MC, et al. 2016. Genomic analyses identify molecular subtypes of pancreatic cancer. *Nature* **531**: 47–52.

Baradaran B, Shahbazi R, Khordadmehr M. 2019. Dysregulation of key microRNAs in pancreatic cancer development. *Biomed Pharmacother* **109**: 1008–1015.

Boutet SC, Cheung TH, Quach NL, Liu L, Prescott SL, Edalati A, Iori K, Rando TA. 2012. Alternative polyadenylation mediates microRNA regulation of muscle stem cell function. *Cell Stem Cell* **10**: 327–36.

Brett-Morris A, Wright BM, Seo Y, Pasupuleti V, Zhang J, Lu J, Spina R, Bar EE, Gujrati M, Schur R, et al. 2014. The Polyamine Catabolic Enzyme SAT1 Modulates Tumorigenesis and Radiation Response in GBM. *Cancer Res* **74**: 6925–6934.

Brumbaugh J, Di Stefano B, Wang X, Borkent M, Forouzmand E, Clowers KJ, Ji F, Schwarz BA, Kalocsay M, Elledge SJ, et al. 2018. Nudt21 Controls Cell Fate by Connecting Alternative Polyadenylation to Chromatin Signaling. *Cell* **172**: 106–120.

Cai J, Li R, Xu X, Zhang L, Lian R, Fang L, Huang Y, Feng X, Liu X, Li X, et al. 2018. CK1α suppresses lung tumour growth by stabilizing PTEN and inducing autophagy. *Nat Cell Biol* **20**: 465–478.

Capello M, Ferri-Borgogno S, Riganti C, Chattaragada MS, Principe M, Roux C, Zhou W, Petricoin EF, Cappello P, Novelli F. 2016. Targeting the Warburg effect in cancer cells through ENO1 knockdown rescues oxidative phosphorylation and induces growth arrest. *Oncotarget* **7**: 5598.

Chen M, Lyu G, Han M, Nie H, Shen T, Chen W, Niu Y, Song Y, Li X, Li H, et al. 2018a. 3’ UTR lengthening as a novel mechanism in regulating cellular senescence. *Genome Res* **28**: 285–294.

Chen X, Zhang J-X, Luo J-H, Wu S, Yuan G-J, Ma N-F, Feng Y, Cai M-Y, Chen R-X, Lu J, et al. 2018b. CSTF2-Induced Shortening of the RAC1 3’UTR Promotes the Pathogenesis of Urothelial Carcinoma of the Bladder. *Cancer Res* **78**: 5848–5862.

Chien Y, White MA. 2003. RAL GTPases are linchpin modulators of human tumour-cell proliferation and survival. *EMBO Rep* **4**: 800–806.

797 Chu Y, Elrod N, Wang C, Li L, Chen T, Routh A, Xia Z, Li W, Wagner EJ, Ji P. 2019. Nudt21
798 regulates the alternative polyadenylation of Pak1 and is predictive in the prognosis of
799 glioblastoma patients. *Oncogene* **38**: 4154–4168.
800 Collisson EA, Sadanandam A, Olson P, Gibb WJ, Truitt M, Gu S, Cooc J, Weinkle J, Kim GE,
801 Jakkula L, et al. 2011. Subtypes of pancreatic ductal adenocarcinoma and their differing
802 responses to therapy. *Nat Med* **17**: 500–503.
803 D Antonio M, Weghorn D, D Antonio-Chronowska A, Coulet F, Olson KM, DeBoever C, Drees
804 F, Arias A, Alakus H, Richardson AL, et al. 2017. Identifying DNase I hypersensitive sites
805 as driver distal regulatory elements in breast cancer. *Nat Commun* **8**: 436.
806 Dangi-Garimella S, Strouch MJ, Grippo PJ, Bentrem DJ, Munshi HG. 2011. Collagen regulation
807 of let-7 in pancreatic cancer involves TGF-β1-mediated membrane type 1-matrix
808 metalloproteinase expression. *Oncogene* **30**: 1002–8.
809 Dey P, Rachagani S, Vaz AP, Ponnusamy MP, Batra SK. 2014. PD2/Paf1 depletion in
810 pancreatic acinar cells promotes acinar-to-ductal metaplasia. *Oncotarget* **5**: 4480–91.
811 Easwaran H, Tsai H-C, Baylin SB. 2014. Cancer epigenetics: tumor heterogeneity, plasticity of
812 stem-like states, and drug resistance. *Mol Cell* **54**: 716–27.
813 Eisenberg E, Levanon EY. 2013. Human housekeeping genes, revisited. *Trends Genet* **29**:
814 569–574.
815 Eisenberg E, Levanon EY. 2003. Human housekeeping genes are compact. *Trends Genet* **19**:
816 362–5.
817 Elkon R, Ugalde AP, Agami R. 2013. Alternative cleavage and polyadenylation: extent,
818 regulation and function. *Nat Rev Genet* **14**: 496–506.
819 Erson-Bensan AE, Can T. 2016. Alternative Polyadenylation: Another Foe in Cancer. *Mol*
820 *Cancer Res* **14**: 507–517.
821 Fahrmann JF, Bantis LE, Capello M, Scelo G, Dennison JB, Patel N, Murage E, Vykoukal J,
822 Kundnani DL, Foretova L, et al. 2018. A Plasma-Derived Protein-Metabolite Multiplexed
823 Panel for Early-Stage Pancreatic Cancer. *JNCI J Natl Cancer Inst* **111**: 1–8.
824 Fan J, Lv J. 2008. Sure independence screening for ultrahigh dimensional feature space. *J R*
825 *Stat Soc Ser B* **70**: 849–911.
826 Feigin ME, Garvin T, Bailey P, Waddell N, Chang DK, Kelley DR, Shuai S, Gallinger S,
827 McPherson JD, Grimmond SM, et al. 2017. Recurrent noncoding regulatory mutations in
828 pancreatic ductal adenocarcinoma. *Nat Genet* **49**: 825–833.
829 Feng X, Li L, Wagner EJ, Li W. 2017. TC3A: The Cancer 3′ UTR Atlas. *Nucleic Acids Res* **46**:
830 D1027–D1030.

Grassi E, Mariella E, Lembo A, Molineris I, Provero P. 2016. Roar: detecting alternative polyadenylation with standard mRNA sequencing libraries. *BMC Bioinformatics* **17**: 423.

Gruber AJ, Zavolan M. 2019. Alternative cleavage and polyadenylation in health and disease. *Nat Rev Genet* **20**: 599–614.

Hinohara K, Polyak K. 2019. Intratumoral Heterogeneity: More Than Just Mutations. *Trends Cell Biol* **29**: 569–579.

Hsu C-C, Leu Y-W, Tseng M-J, Lee K-D, Kuo T-Y, Yen J-Y, Lai Y-L, Hung Y-C, Sun W-S, Chen C-M, et al. 2011. Functional characterization of Trip10 in cancer cell growth and survival. *J Biomed Sci* **18**: 12.

Hu Y, Ou Y, Wu K, Chen Y, Sun W. 2012. miR-143 inhibits the metastasis of pancreatic cancer and an associated signaling pathway. *Tumor Biol* **33**: 1863–1870.

Järås M, Miller PG, Chu LP, Puram R V, Fink EC, Schneider RK, Al-Shahrour F, Peña P, Breyfogle LJ, Hartwell KA, et al. 2014. Csnk1a1 inhibition has p53-dependent therapeutic efficacy in acute myeloid leukemia. *J Exp Med* **211**: 605–12.

Ji S, Zhang B, Liu J, Qin Y, Liang C, Shi S, Jin K, Liang D, Xu W, Xu H, et al. 2016. ALDOA functions as an oncogene in the highly metastatic pancreatic cancer. *Cancer Lett* **374**: 127–135.

Jiang S, Zhang M, Sun J, Yang X. 2018. Casein kinase 1α: biological mechanisms and theranostic potential. *Cell Commun Signal* **16**: 23.

Jones S, Anagnostou V, Lytle K, Parpart-Li S, Nesselbush M, Riley DR, Shukla M, Chesnick B, Kadan M, Papp E, et al. 2015. Personalized genomic analyses for cancer mutation discovery and interpretation. *Sci Transl Med* **7**: 283ra53.

Jones S, Zhang X, Parsons DW, Lin JC-H, Leary RJ, Angenendt P, Mankoo P, Carter H, Kamiyama H, Jimeno A, et al. 2008. Core signaling pathways in human pancreatic cancers revealed by global genomic analyses. *Science* **321**: 1801–6.

Kent OA, Chivukula RR, Mullendore M, Wentzel EA, Feldmann G, Lee KH, Liu S, Leach SD, Maitra A, Mendell JT. 2010. Repression of the miR-143/145 cluster by oncogenic Ras initiates a tumor-promoting feed-forward pathway. *Genes Dev* **24**: 2754–2759.

Kent OA, McCall MN, Cornish TC, Halushka MK. 2014. Lessons from miR-143/145: the importance of cell-type localization of miRNAs. *Nucleic Acids Res* **42**: 7528–7538.

Khurana E, Fu Y, Colonna V, Mu XJ, Kang HM, Lappalainen T, Sboner A, Lochovsky L, Chen J, Harmanci A, et al. 2013. Integrative annotation of variants from 1092 humans: application to cancer genomics. *Science* **342**: 1235587.

Knippschild U, Gocht A, Wolff S, Huber N, Löhler J, Stöter M. 2005. The casein kinase 1 family:

participation in multiple cellular processes in eukaryotes. *Cell Signal* **17**: 675–689.

Kojima S, Chiyomaru T, Kawakami K, Yoshino H, Enokida H, Nohata N, Fuse M, Ichikawa T, Naya Y, Nakagawa M, et al. 2012. Tumour suppressors miR-1 and miR-133a target the oncogenic function of purine nucleoside phosphorylase (PNP) in prostate cancer. *Br J Cancer* **106**: 405–413.

Kosti I, Jain N, Aran D, Butte AJ, Sirota M. 2016. Cross-tissue Analysis of Gene and Protein Expression in Normal and Cancer Tissues. *Sci Rep* **6**: 24799.

Lackford B, Yao C, Charles GM, Weng L, Zheng X, Choi E-A, Xie X, Wan J, Xing Y, Freudenberg JM, et al. 2014. Fip1 regulates mRNA alternative polyadenylation to promote stem cell self-renewal. *EMBO J* **33**: 878–889.

Lantermann AB, Chen D, McCutcheon K, Hoffman G, Frias E, Ruddy D, Rakiec D, Korn J, McAllister G, Stegmeier F, et al. 2015. Inhibition of Casein Kinase 1 Alpha Prevents Acquired Drug Resistance to Erlotinib in EGFR-Mutant Non-Small Cell Lung Cancer. *Cancer Res* **75**: 4937–4948.

Lappalainen T, Sammeth M, Friedländer MR, 'T Hoen PAC, Monlong J, Rivas MA, Gonzàlez-Porta M, Kurbatova N, Griebel T, Ferreira PG, et al. 2013. Transcriptome and genome sequencing uncovers functional variation in humans. *Nature* **501**: 506–511.

Le Pera L, Mazzapioda M, Tramontano A. 2015. 3USS: a web server for detecting alternative 3'UTRs from RNA-seq experiments. *Bioinformatics* **31**: 1845–7.

Lee YS, Dutta A. 2007. The tumor suppressor microRNA let-7 represses the HMGA2 oncogene. *Genes Dev* **21**: 1025–1030.

Li C, Yu S, Nakamura F, Yin S, Xu J, Petrolla AA, Singh N, Tartakoff A, Abbott DW, Xin W, et al. 2009. Binding of pro-prion to filamin A disrupts cytoskeleton and correlates with poor prognosis in pancreatic cancer. *J Clin Invest* **119**: 2725–2736.

Li L, Wang D, Xue M, Mi X, Liang Y, Wang P. 2015. 3′UTR shortening identifies high-risk cancers with targeted dysregulation of the ceRNA network. *Sci Rep* **4**: 5406.

Lianoglou S, Garg V, Yang JL, Leslie CS, Mayr C. 2013. Ubiquitously transcribed genes use alternative polyadenylation to achieve tissue-specific expression. *Genes Dev* **27**: 2380–2396.

Lomberk G, Blum Y, Nicolle R, Nair A, Gaonkar KS, Marisa L, Mathison A, Sun Z, Yan H, Elarouci N, et al. 2018. Distinct epigenetic landscapes underlie the pathobiology of pancreatic cancer subtypes. *Nat Commun* **9**: 1978.

Masamha CP, Xia Z, Yang J, Albrecht TR, Li M, Shyu A-B, Li W, Wagner EJ. 2014. CFIm25 links alternative polyadenylation to glioblastoma tumour suppression. *Nature* **510**: 412–

416.

Matoulkova E, Michalova E, Vojtesek B, Hrstka R. 2012. The role of the 3' untranslated region in post-transcriptional regulation of protein expression in mammalian cells. *RNA Biol* **9**: 563–576.

Maurer C, Holmstrom SR, He J, Laise P, Su T, Ahmed A, Hibshoosh H, Chabot JA, Oberstein PE, Sepulveda AR, et al. 2019. Experimental microdissection enables functional harmonisation of pancreatic cancer subtypes. *Gut* **68**: 1034–1043.

Maurer HC, Olive KP. 2019. Laser capture microdissection on frozen sections for extraction of high-quality nucleic acids. *Methods Mol Biol* **1882**: 253–259.

Mayr C. 2016. Evolution and Biological Roles of Alternative 3'UTRs. *Trends Cell Biol* **26**: 227–237.

Mayr C. 2018. What Are 3 ′ UTRs Doing? *Cold Spring Harb Perspect Biol*.

Mayr C, Bartel DP. 2009. Widespread Shortening of 3′UTRs by Alternative Cleavage and Polyadenylation Activates Oncogenes in Cancer Cells. *Cell* **138**: 673–684.

Mayr C, Hemann MT, Bartel DP. 2007. Disrupting the Pairing Between let-7 and Hmga2 Enhances Oncogenic Transformation. *Science* **315**: 1576–1579.

McGranahan N, Swanton C. 2017. Clonal Heterogeneity and Tumor Evolution: Past, Present, and the Future. *Cell* **168**: 613–628.

Mihaljevic AL, Michalski CW, Friess H, Kleeff J. 2010. Molecular mechanism of pancreatic cancer—understanding proliferation, invasion, and metastasis. *Langenbeck's Arch Surg* **395**: 295–308.

Miles WO, Lembo A, Volorio A, Brachtel E, Tian B, Sgroi D, Provero P, Dyson N. 2016. Alternative Polyadenylation in Triple-Negative Breast Tumors Allows NRAS and c-JUN to Bypass PUMILIO Posttranscriptional Regulation. *Cancer Res* **76**: 7231–7241.

Mitra M, Johnson EL, Swamy VS, Nersesian LE, Corney DC, Robinson DG, Taylor DG, Ambrus AM, Jelinek D, Wang W, et al. 2018. Alternative polyadenylation factors link cell cycle to migration. *Genome Biol* **19**: 176.

Moffitt RA, Marayati R, Flate EL, Volmar KE, Loeza SGH, Hoadley KA, Rashid NU, Williams LA, Eaton SC, Chung AH, et al. 2015. Virtual microdissection identifies distinct tumor- and stroma-specific subtypes of pancreatic ductal adenocarcinoma. *Nat Genet* **47**: 1168–1178.

Nimmakayala RK, Seshacharyulu P, Lakshmanan I, Rachagani S, Chugh S, Karmakar S, Rauth S, Vengoji R, Atri P, Talmon GA, et al. 2018. Cigarette Smoke Induces Stem Cell Features of Pancreatic Cancer Cells via PAF1. *Gastroenterology* **155**: 892–908.e6.

Noone A, Howlader N, Krapcho M, Miller D, Brest A, Yu M, Ruhl J, Tatalovich Z, Mariotto A,

Lewis D, et al. 2019. *Survival Rates for Pancreatic Cancer*. American Cancer Society, Atlanta, GA.

Park HJ, Ji P, Kim S, Xia Z, Rodriguez B, Li L, Su J, Chen K, Masamha CP, Baillat D, et al. 2018. 3′ UTR shortening represses tumor-suppressor genes in trans by disrupting ceRNA crosstalk. *Nat Genet* **50**: 783–789.

Passacantilli I, Panzeri V, Bielli P, Farini D, Pilozzi E, Fave GD, Capurso G, Sette C. 2017. Alternative polyadenylation of ZEB1 promotes its translation during genotoxic stress in pancreatic cancer cells. *Cell Death Dis* **8**: e3168.

Pereira B, Billaud M, Almeida R. 2017. RNA-Binding Proteins in Cancer: Old Players and New Actors. *Trends in cancer* **3**: 506–528.

Pham H, Rodriguez CE, Donald GW, Hertzer KM, Jung XS, Chang H-H, Moro A, Reber HA, Hines OJ, Eibl G. 2013. miR-143 decreases COX-2 mRNA stability and expression in pancreatic cancer cells. *Biochem Biophys Res Commun* **439**: 6–11.

Phanstiel O. 2018. An overview of polyamine metabolism in pancreatic ductal adenocarcinoma. *UICC Int J Cancer IJC* **142**: 1968–1976.

Proudfoot NJ. 2011. Ending the message: poly(A) signals then and now. *Genes Dev* **25**: 1770–82.

Qin Y, Dang X, Li W, Ma Q. 2014. miR-133a Functions as a Tumor Suppressor and Directly Targets FSCN1 in Pancreatic Cancer. *Oncol Res Featur Preclin Clin Cancer Ther* **21**: 353–363.

Quinlan AR, Hall IM. 2010. BEDTools: a flexible suite of utilities for comparing genomic features. *Bioinformatics* **26**: 841–842.

R Core Team. 2014. R: A language and environment for statistical computing. R Foundation for Statistical Computing, Vienna, Austria.

Raphael B, Aguirre A, The Cancer Genome Atlas. 2017. Integrated Genomic Characterization of Pancreatic Ductal Adenocarcinoma. *Cancer Cell* **32**: 185–203.

Rena G, Bain J, Elliott M, Cohen P. 2004. D4476, a cell-permeant inhibitor of CK1, suppresses the site-specific phosphorylation and nuclear exclusion of FOXO1a. *EMBO Rep* **5**: 60–65.

Rheinbay E, Parasuraman P, Grimsby J, Tiao G, Engreitz JM, Kim J, Lawrence MS, Taylor-Weiner A, Rodriguez-Cuevas S, Rosenberg M, et al. 2017. Recurrent and functional regulatory mutations in breast cancer. *Nature* **547**: 55–60.

Sandberg R, Neilson JR, Sarma A, Sharp PA, Burge CB. 2008. Proliferating cells express mRNAs with shortened 3’ untranslated regions and fewer microRNA target sites. *Science* **320**: 1643–7.

967 Schittek B, Sinnberg T. 2014. Biological functions of casein kinase 1 isoforms and putative roles
968 in tumorigenesis. *Mol Cancer* **13**: 231.
969 Schultz NA, Dehlendorff C, Jensen B V., Bjerregaard JK, Nielsen KR, Bojesen SE, Calatayud D,
970 Nielsen SE, Yilmaz M, Holländer NH, et al. 2014. MicroRNA Biomarkers in Whole Blood for
971 Detection of Pancreatic Cancer. *JAMA* **311**: 392.
972 Seshacharyulu P, Pandey P, Datta K, Batra SK. 2013. Phosphatase: PP2A structural
973 importance, regulation and its aberrant expression in cancer. *Cancer Lett* **335**: 9–18.
974 Shi Y, Manley JL. 2015. The end of the message: multiple protein-RNA interactions define the
975 mRNA polyadenylation site. *Genes Dev* **29**: 889–97.
976 Sinnberg T, Menzel M, Kaesler S, Biedermann T, Sauer B, Nahnsen S, Schwarz M, Garbe C,
977 Schittek B. 2010. Suppression of Casein Kinase 1 in Melanoma Cells Induces a Switch
978 in -Catenin Signaling to Promote Metastasis. *Cancer Res* **70**: 6999–7009.
979 Tan S, Li H, Zhang W, Shao Y, Liu Y, Guan H, Wu J, Kang Y, Zhao • Junsong, Yu Q, et al.
980 2018. NUDT21 negatively regulates PSMB2 and CXXC5 by alternative polyadenylation
981 and contributes to hepatocellular carcinoma suppression. *Oncogene* **37**: 4887–4900.
982 The Cancer Genome Atlas, Chang K, Creighton CJ, Davis C, Donehower L, Drummond J,
983 Wheeler D, Ally A, Balasundaram M, Birol I, et al. 2013. The Cancer Genome Atlas Pan-
984 Cancer analysis project. *Nat Genet* **45**: 1113.
985 The GTEx Consortium. 2015. The Genotype-Tissue Expression (GTEx) pilot analysis:
986 Multitissue gene regulation in humans. *Science* **348**: 648–660.
987 Tian B, Manley JL. 2017. Alternative polyadenylation of mRNA precursors. *Nat Rev Mol Cell*
988 *Biol* **18**: 18–30.
989 Tiriac H, Belleau P, Engle DD, Plenker D, Deschênes A, Somerville TDD, Froeling FEM,
990 Burkhart RA, Denroche RE, Jang G-H, et al. 2018. Organoid Profiling Identifies Common
991 Responders to Chemotherapy in Pancreatic Cancer. *Cancer Discov* **8**: 1112–1129.
992 Tsai W-C, Hsu PW-C, Lai T-C, Chau G-Y, Lin C-W, Chen C-M, Lin C-D, Liao Y-L, Wang J-L,
993 Chau Y-P, et al. 2009. MicroRNA-122, a tumor suppressor microRNA that regulates
994 intrahepatic metastasis of hepatocellular carcinoma. *Hepatology* **49**: 1571–1582.
995 Vandenberg CA. 2008. Integrins step up the pace of cell migration through polyamines and
996 potassium channels. *Proc Natl Acad Sci U S A* **105**: 7109–10.
997 Vaz AP, Ponnusamy MP, Rachagani S, Dey P, Ganti AK, Batra SK. 2014. Novel role of
998 pancreatic differentiation 2 in facilitating self-renewal and drug resistance of pancreatic
999 cancer stem cells. *Br J Cancer* **111**: 486–496.
1000 Waddell N, Pajic M, Patch A-M, Chang DK, Kassahn KS, Bailey P, Johns AL, Miller D, Nones K,

Quek K, et al. 2015. Whole genomes redefine the mutational landscape of pancreatic cancer. *Nature* **518**: 495–501.

Wang Q, Wang J, Niu S, Wang S, Liu Y, Wang X, Wang S, Wang S, Liu Y, Liu Y, et al. 2019. MicroRNA-664 targets paired box protein 6 to inhibit the oncogenicity of pancreatic ductal adenocarcinoma. *Int J Oncol* **54**: 1884–1896.

Wang X, Lu X, Zhang T, Wen C, Shi M, Tang X, Chen H, Peng C, Li H, Fang Y, et al. 2016. mir-329 restricts tumor growth by targeting grb2 in pancreatic cancer. *Oncotarget* **7**: 21441–53.

Weinhold N, Jacobsen A, Schultz N, Sander C, Lee W. 2014. Genome-wide analysis of noncoding regulatory mutations in cancer. *Nat Genet* **46**: 1160–1165.

Wu D-H, Liang H, Lu S-N, Wang H, Su Z-L, Zhang L, Ma J-Q, Guo M, Tai S, Yu S. 2018. miR-124 Suppresses Pancreatic Ductal Adenocarcinoma Growth by Regulating Monocarboxylate Transporter 1-Mediated Cancer Lactate Metabolism. *Cell Physiol Biochem* **50**: 924–935.

Xia Z, Donehower LA, Cooper TA, Neilson JR, Wheeler DA, Wagner EJ, Li W. 2014. Dynamic analyses of alternative polyadenylation from RNA-seq reveal a 3′-UTR landscape across seven tumour types. *Nat Commun* **5**: 5274.

Xiang Y, Ye Y, Lou Y, Yang Y, Cai C, Zhang Z, Mills T, Chen N-Y, Kim Y, Muge Ozguc F, et al. 2018. Comprehensive Characterization of Alternative Polyadenylation in Human Cancer. *JNCI J Natl Cancer Inst* **110**: 379–389.

Xue Z, Warren RL, Gibb EA, MacMillan D, Wong J, Chiu R, Hammond SA, Yang C, Nip KM, Ennis CA, et al. 2018. Recurrent tumor-specific regulation of alternative polyadenylation of cancer-related genes. *BMC Genomics* **19**: 536.

Yaffe MB. 2019. Why geneticists stole cancer research even though cancer is primarily a signaling disease. *Sci Signal* **12**: eaaw3483.

Ye C, Long Y, Ji G, Li QQ, Wu X, Berger B. 2018. APAtrap: identification and quantification of alternative polyadenylation sites from RNA-seq data ed. B. Berger. *Bioinformatics*.

Yong TJ, Gan YY, Toh BH, Sentry JW. 2000. Human CKIalpha(L) and CKIalpha(S) are encoded by both 2.4- and 4. 2-kb transcripts, the longer containing multiple RNA-destablising elements. *Biochim Biophys Acta* **1492**: 425–33.

Yu S, Li L, Wu Q, Dou N, Li Y, Gao Y, Dou N, Dou N, Li Y, Li Y, et al. 2018. PPP2R2D, a regulatory subunit of protein phosphataseï¿½2A, promotes gastric cancer growth and metastasis via mechanistic target of rapamycin activation. *Int J Oncol* **52**: 2011–2020.

Zeng WZD, Glicksberg BS, Li Y, Chen B. 2019. Selecting precise reference normal tissue samples for cancer research using a deep learning approach. *BMC Med Genomics* **12**: 21.

Zhang Y, Li M, Wang H, Fisher WE, Lin PH, Yao Q, Chen C. 2009. Profiling of 95 MicroRNAs in Pancreatic Cancer Cell Lines and Surgical Specimens by Real-Time PCR Analysis. *World J Surg* **33**: 698–709.

Zhou A-X, Toylu A, Nallapalli RK, Nilsson G, Atabey N, Heldin C-H, Borén J, Bergo MO, Akyürek LM. 2011. Filamin a mediates HGF/c-MET signaling in tumor cell migration. *Int J Cancer* **128**: 839–846.

Zhu J, He F, Song S, Wang J, Yu J. 2008. How many human genes can be defined as housekeeping with current expression data? *BMC Genomics* **9**: 172.

Venkat S, *et al.*, Figure 1

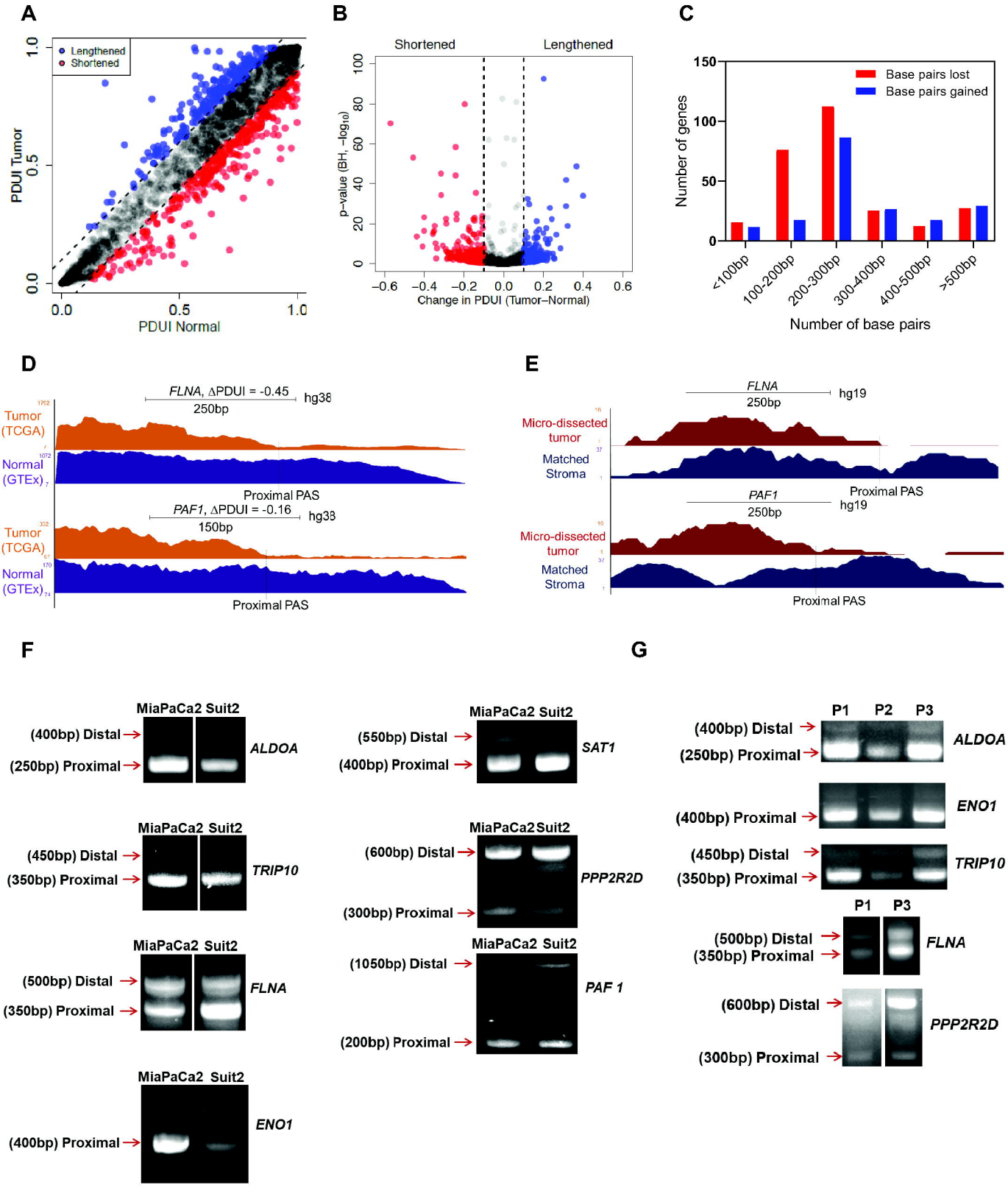

Venkat S, *et al.*, Figure 2

A

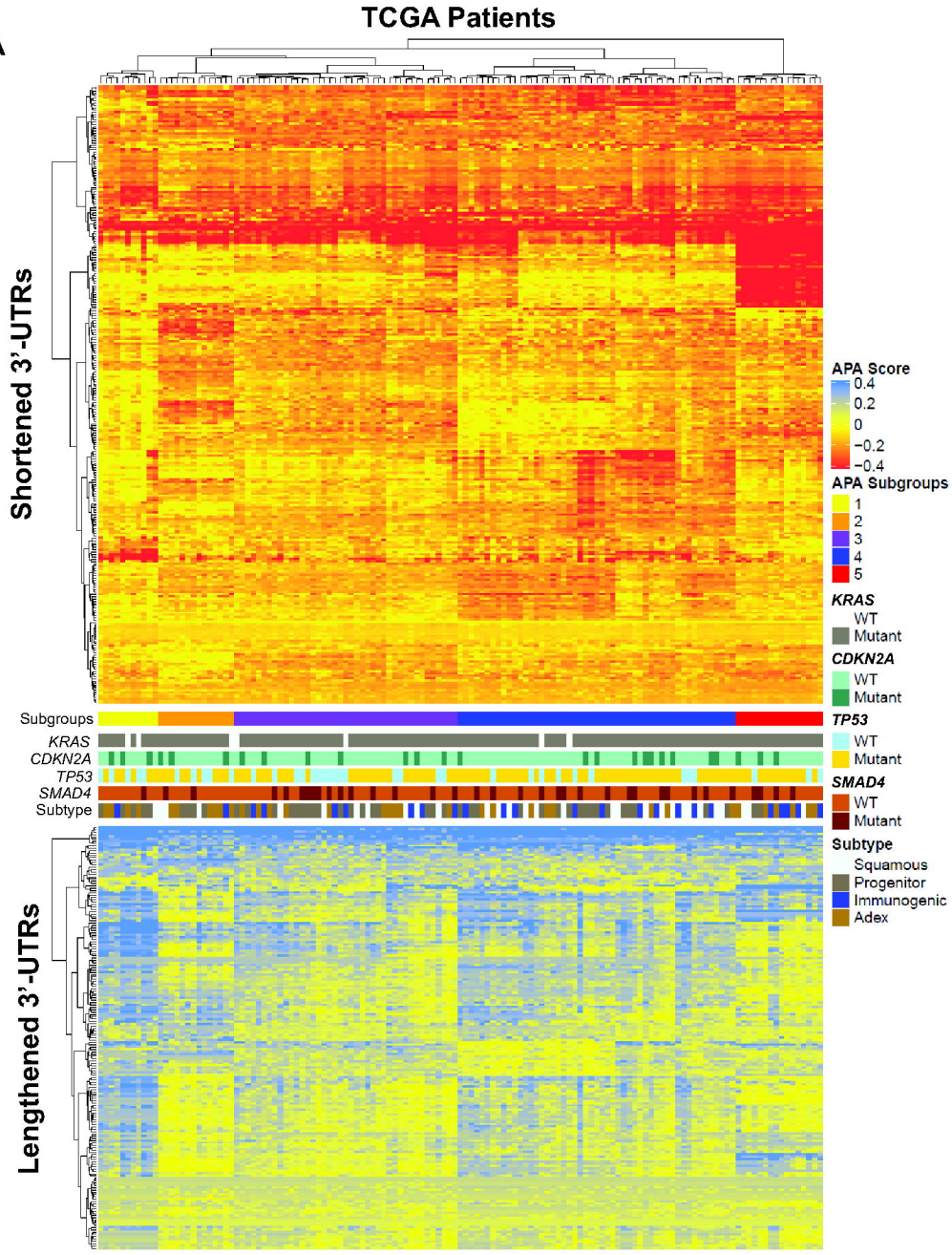

B

Regulatory process	# Genes altered	FDR	Representative genes
Metabolism of proteins	107	2.62E-13	*EIF5A, HSPD1, MRPL32, ADD1*
Membrane Trafficking	40	1.61E-06	*STX10, USO1, COPB1, M6PR*
mRNA Splicing	17	3.89E-04	*HNRNPA1, SRSF11, PABPN1, SYMPK*
mRNA 3'-end processing	9	1.30E-03	*SRSF1, SRSF2, CHTOP, NCBP2*
Platelet activation and signaling	20	4.26E-04	*SERPINA1, FLNA, CFL1, ALDOA*
Smooth Muscle Contraction	6	1.13E-02	*CALM1, ANXA2, MYL6, TPM1*
Signaling by Receptor Tyrosine Kinases	26	1.26E-03	*VAV2, BCAR1, RAP1B, CDC42*
Signaling by RHO GTPases	5	1.03E-02	*CALM1, MYL12B, CDC42, FLNA*
JAK-STAT signaling	7	1.84E-02	*ANXA2, CDC42, RAP1B, PPIA*
Cell-extracellular matrix interactions	4	3.87E-02	*VASP, ACTN1, FLNA, FBLIM1*
Cell cycle	18	4.69E-02	*BUB3, PPP2R2D, SET, RAB2A*

Venkat S, *et al.*, Figure 3

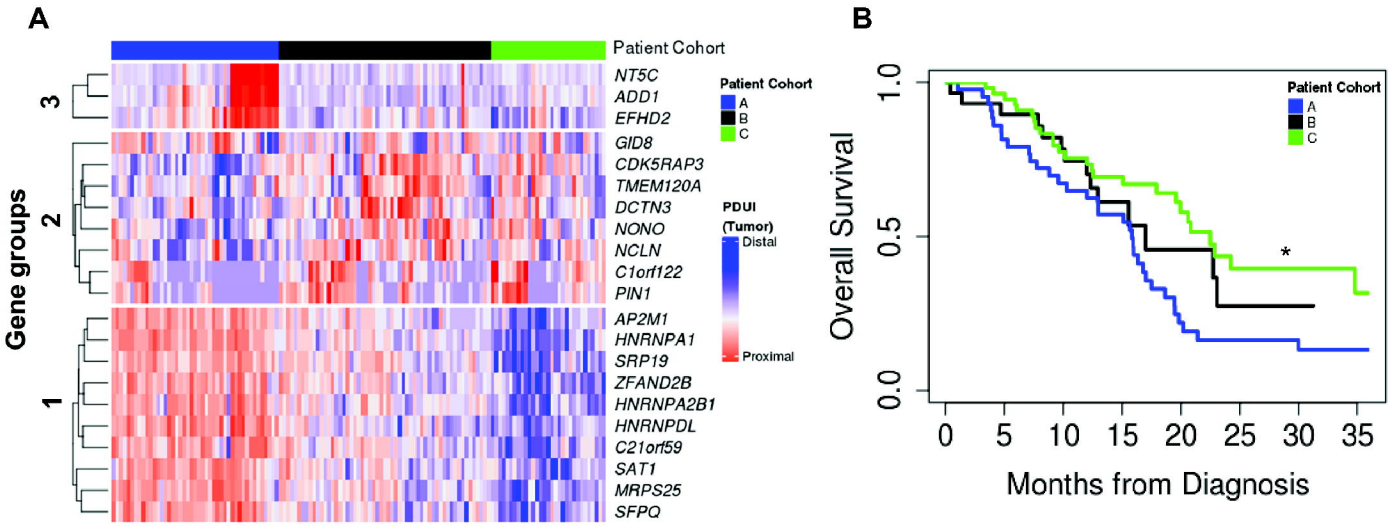

Venkat S, *et al.*, Figure 4

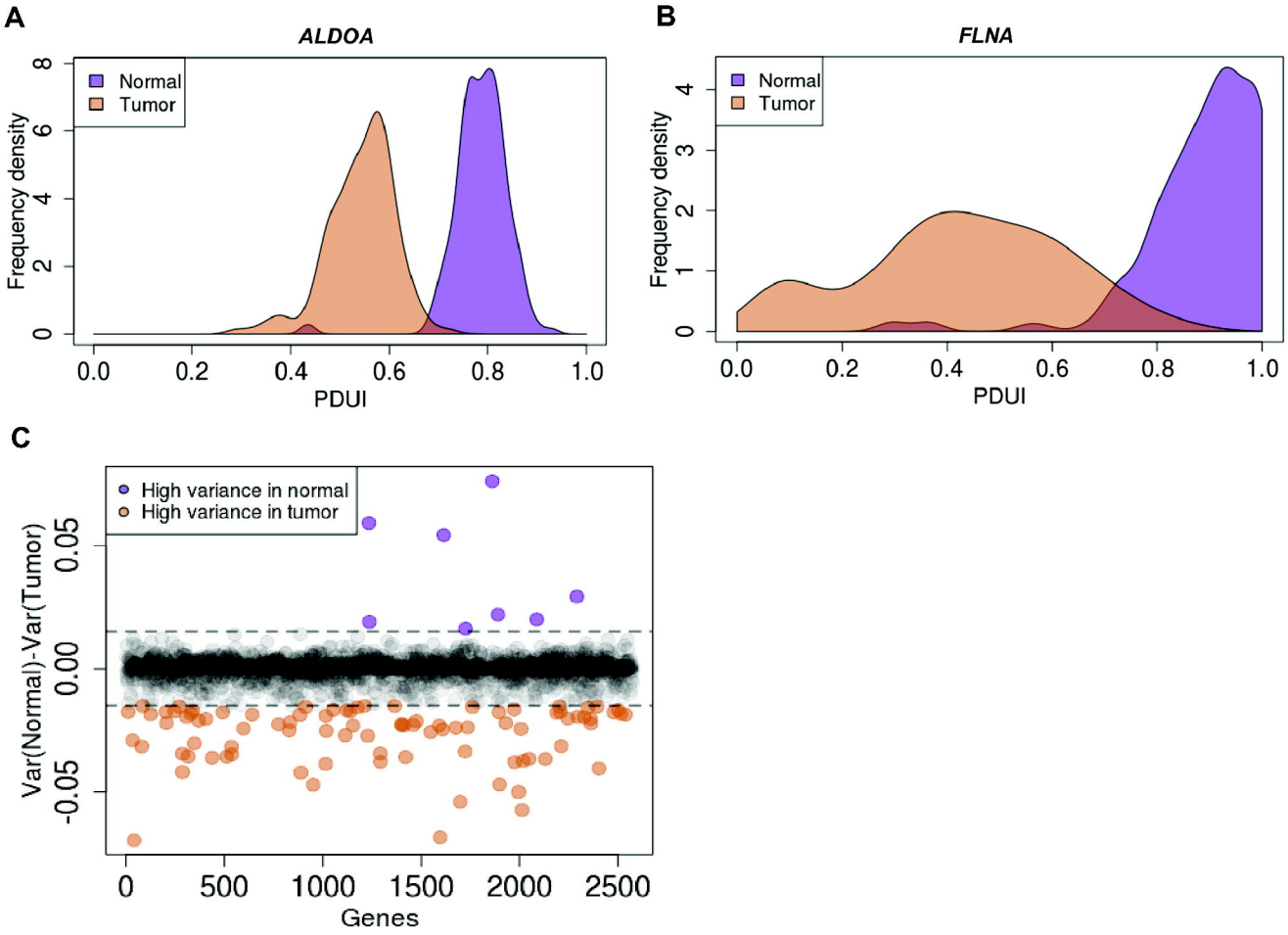

Venkat S, *et al.*, Figure 5

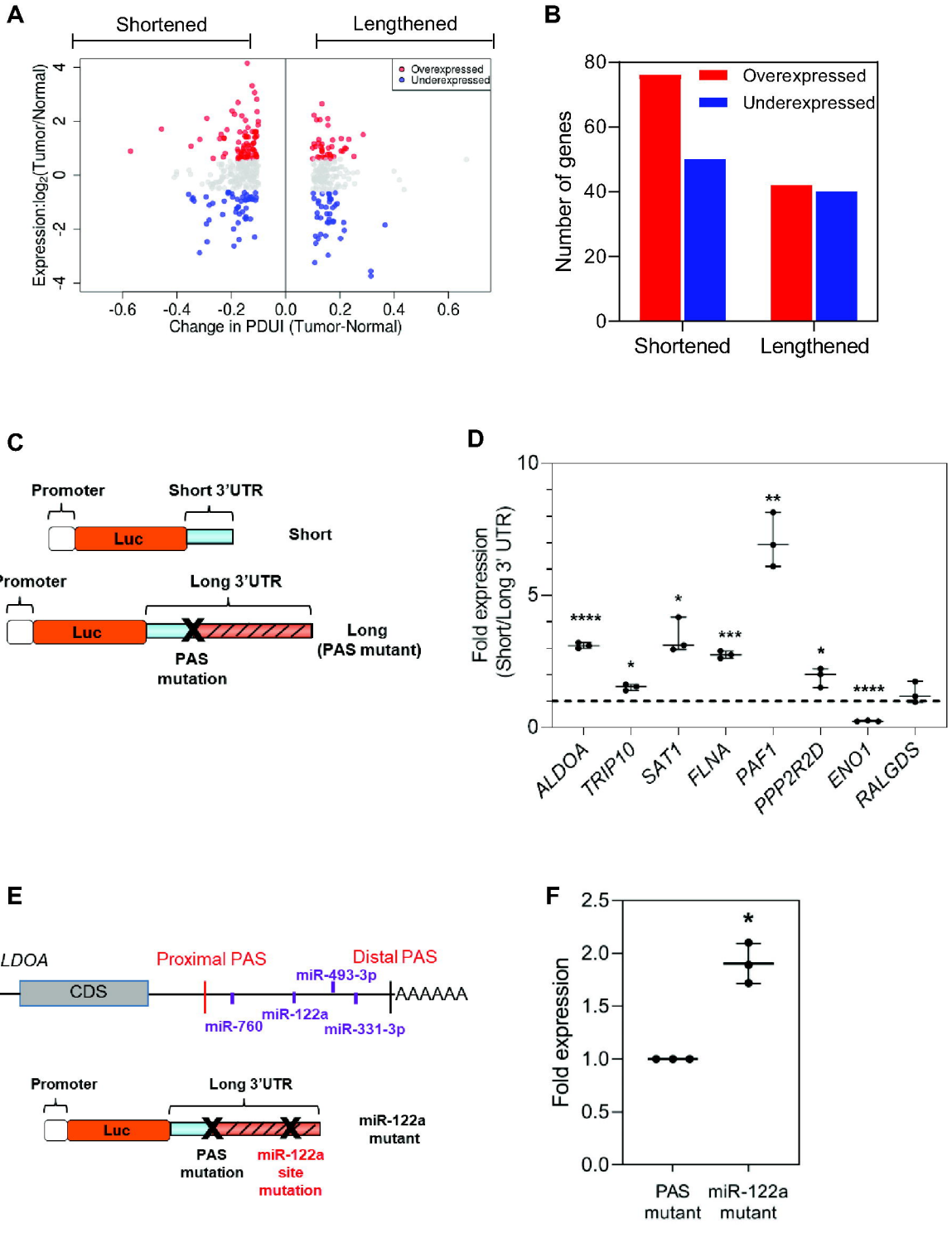

Venkat S, *et al.*, Figure 6

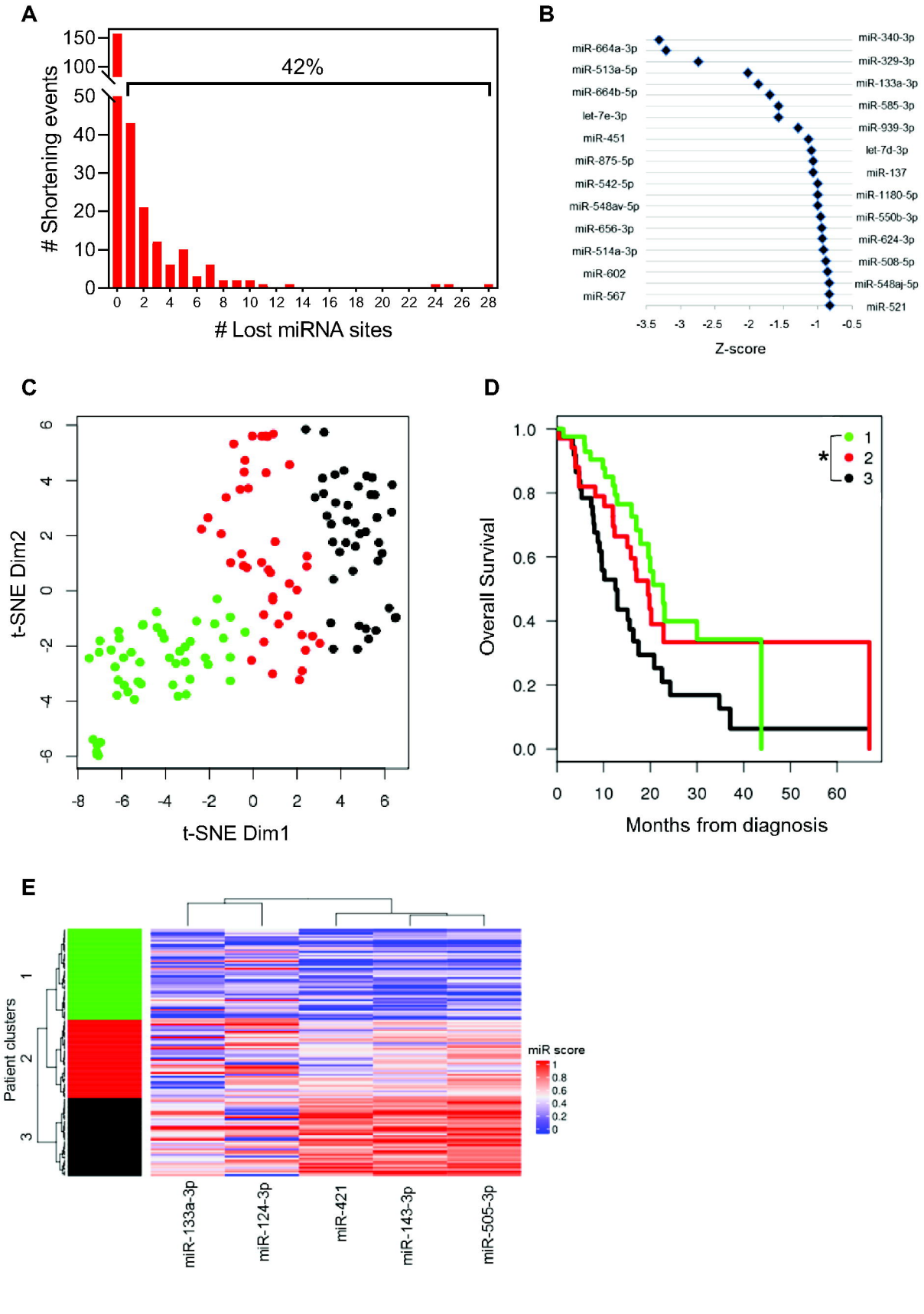

Venkat S, *et al.*, Figure 7